Hindawi Publishing Corporation
Journal of Nanomaterials
Volume 2016, Article ID 7148307, 5 pages
http://dx.doi.org/10.1155/2016/7148307

Research Article

Microwave-Assisted Hydrothermal Synthesis and Annealing of DyF_3 Nanoparticles

E. M. Alakshin,[1] A. V. Klochkov,[1] E. I. Kondratyeva,[1] S. L. Korableva,[1] A. G. Kiiamov,[1] D. S. Nuzhina,[1] A. A. Stanislavovas,[1] M. S. Tagirov,[1,2] M. Yu. Zakharov,[1] and S. Kodjikian[3]

[1]*Kazan Federal University, Kremlevskaya 18, 420008 Kazan, Russia*
[2]*Institute of Perspective Research, TAS, L. Bulachnaya 36a, 420111 Kazan, Russia*
[3]*University Grenoble Alpes, CNRS, Institut NEEL, 38000 Grenoble, France*

Correspondence should be addressed to E. M. Alakshin; alakshin@gmail.com

Received 14 June 2016; Revised 14 October 2016; Accepted 24 October 2016

Academic Editor: Paulo Cesar Morais

The series of DyF_3 nanosized samples was synthesized by the colloidal chemistry method. The microwave-assisted hydrothermal treatment was used for the first time for the modification of DyF_3 nanoparticles. Transmission electron microscopy images show that the DyF_3 nanoparticles have average particle size of about 16–18 nm and the size distribution becomes narrower during the microwave irradiation. The X-ray diffraction analysis shows the narrowing of the diffraction peaks versus microwave treatment time. The experimental data demonstrates restructuring of the nanoparticles and their crystal structure becomes closer to the ideal DyF_3 regular structure during the microwave irradiation of colloidal solution. The defect-annealing model of the microwave-assisted hydrothermal modification process is suggested.

1. Introduction

Several dozen research papers dedicated to LnF_3 nanosized samples synthesis have been published in recent years. Nowadays the lanthanide fluoride nanoparticles attract scientific interest because of their possible applications in many areas such as lasers, biolabels, and optical amplifiers [1–12]. The autoclave hydrothermal treatment is often used for structure and size modification of the lanthanide nanoparticles. The microwave-assisted synthesis of PrF_3 nanoparticles was suggested by Ma et al. [13] and modified at Kazan Federal University (Kazan, Russia). The PrF_3 nanoparticles size and structure dependence on the microwave-assisted hydrothermal treatment time were obtained by the high-resolution transmission electron microscopy (TEM), nuclear magnetic resonance (NMR), and electron paramagnetic resonance [14–21].

The other trifluoride compound of great interest is DyF_3. Recent research showed that DyF_3 powders could significantly improve the properties of Nd-Fe-B magnets [22–25]. In addition, DyF_3 is an important component of oxyfluoride glasses [26]. On the other hand, there is a ferromagnetic phase transition in a single crystal at $T_c = 2.55$ K [27]. Investigation of Curie temperature dependence versus the size of DyF_3 nanoparticles is a fundamental problem. There are only few reports about DyF_3 nanoparticles synthesis [28–30] and the size modification was achieved by the autoclave technique.

The aim of the present work is a synthesis and modification of DyF_3 nanoparticles using the microwave-assisted hydrothermal treatment method.

2. Materials and Methods

Sodium fluoride NaF (99.9%) and dysprosium oxide Dy_2O_3 (99.99%) were obtained from Sigma-Aldrich. The nanosized DyF_3 samples #1–3 were synthesized by similar method as for PrF_3 nanoparticles synthesis [14, 15]. In a typical synthesis, 6.2 g of powdered dysprosium oxide Dy_2O_3 was dissolved in 400 mL of 10% nitric acid HNO_3 aqueous solution to form a transparent solution

$$\mathrm{Dy_2O_3\,(s) + 6HNO_3\,(aq) \longrightarrow 2Dy\,(NO_3)_3\,(aq) + 3H_2O\,(l)} \quad (1)$$

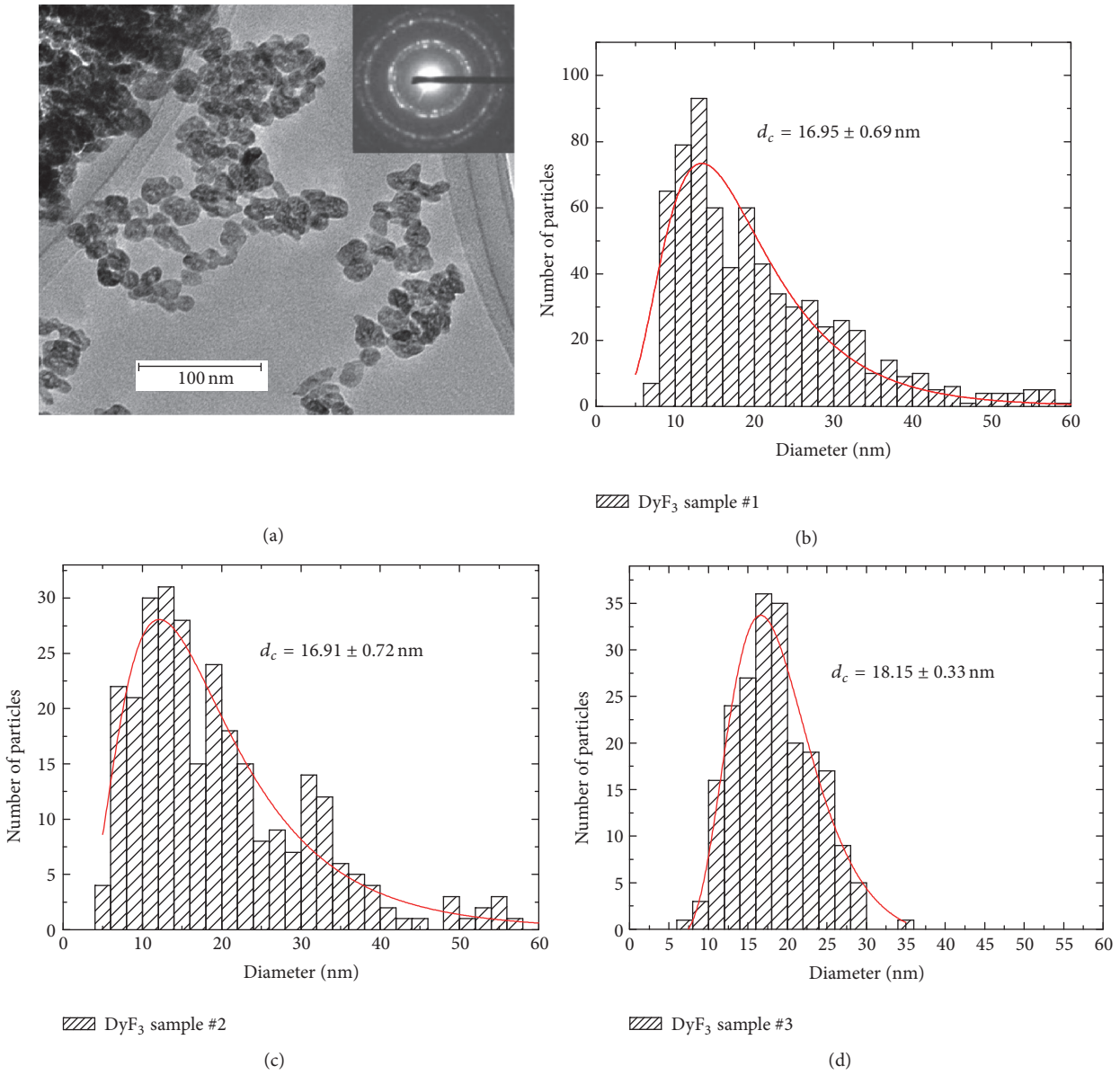

FIGURE 1: (a) TEM image of DyF_3 nanoparticles with corresponding electron diffraction pattern in the insert (sample #3). (b)–(d) The size distribution diagrams for all samples. Solid line is the log-normal distribution fitting, and d_c is the center.

Then, after filtering, 4.75 g of sodium fluoride NaF (F : Dy = 3 : 1) was added into the abovementioned solution under violent stirring. A white colloidal precipitate of DyF_3 appeared immediately.

$$\mathrm{Dy(NO_3)_3\,(aq) + 3NaF\,(s)} \longrightarrow \mathrm{DyF_3\,(s) + 3NaNO_3\,(aq)} \quad (2)$$

The pH of the suspension was adjusted by 25% ammonia aqueous solution (about 4.0–5.0). Deionized water was filled into the suspension to make the volume up to 750 mL. After stirring for about 20 min, the suspension was finally transferred into a 1 L round flask (synthesis of sample #1 has been stopped at this stage). Part of the solution was placed into the microwave oven (650 W, 2.45 GHz) for further hydrothermal treatment (sample #2). The suspension was put into the microwave oven at 70% of the maximum power for 30 minutes. The resulting product was collected by centrifugation (Janetski K24; 12000 RPM) and washed using the deionized water for several times.

Finally, the solution was dried out on the flat surface in air at room temperature. Sample #3 was prepared by the same method and treated by the microwave irradiation for 420 minutes.

TEM images of nanosized samples were obtained by using Philips CM300 operated at 300 kV (Neel Institute, Grenoble, France). Powder X-ray diffraction was done by Bruker D8 Advance X-ray diffractometer with use of copper Ka (α = 1.5418 Å) radiation and continuous scan (scan speed 0.005 degrees per second in the range of diffraction angles 20–60 degrees).

3. Results and Discussion

Figure 1 shows the TEM image with the corresponding electron diffraction pattern in the insert (sample #3) and size

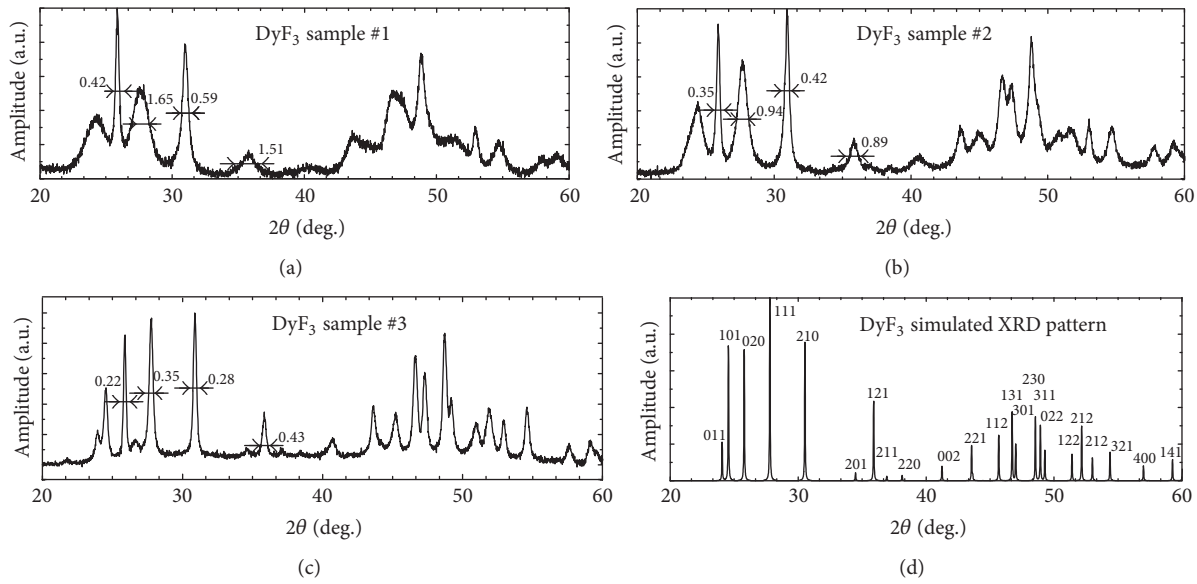

Figure 2: (a)–(c) Experimental XRD patterns of synthesized DyF_3 nanosized samples #1–3. (d) simulated XRD patterns in PowderCell software.

distribution diagrams for all samples. The sharp diffraction rings show the crystal particles presence (rings radii: 0.36 nm, 0.32 nm, and 0.20 nm). All diagrams were fitted by the log-normal distribution. The synthesized nanoparticles have average size of about 16–18 nm (sample #1, 16.9 nm; sample #2, 16.9 nm; sample #3, 18.2 nm). There is no significant DyF_3 nanoparticles size dependence on the microwave-assisted hydrothermal treatment time unlike the case of PrF_3 sample [20]. Clearly, the size distribution becomes narrower during the microwave irradiation. In the case of the microwave-assisted synthesis of PrF_3 nanoparticles, the restructuring of particles was observed earlier by NMR [20]. It was interesting to see the crystal structure changes in the process of DyF_3 nanosized samples treatment.

Crystal structure of DyF_3 nanoparticles was characterized by X-ray diffraction (XRD). Experimental XRD patterns of three DyF_3 nanosized samples are shown in Figure 2. Diffraction peaks could be indexed from the simulated pattern calculated by PowderCell [31] software (space group Pnma (No. 62), lattice constants $a = 0.6460$ nm, $b = 0.6906$ nm, and $c = 0.4376$ nm [32]). Obviously, sample #1 (Figure 2(a)) has wide peaks and after 30 minutes of the microwave-assisted hydrothermal treatment the peaks becomes narrower (Figure 2(b)). After 7 hours of treatment the XRD pattern became even narrower (Figure 2(c)). High and sharp peaks indicate high crystallinity of nanoparticles for sample #3.

The analysis of obtained experimental data suggests the following hypothetical picture of the microwave-assisted hydrothermal modification process. Sample #1 has many defects of crystal structure because of the explosive character of the colloidal reaction. Further microwave treatment of the colloidal solution leads to local heating of DyF_3 particles. Some bigger particles crack into smaller ones, making the size distribution narrower, but the local restructuring continues further. The restructuring leads to decrease in the number of crystal structure defects.

The obtained results of restructuring process are different from that of PrF_3 nanoparticles, where the weak size dependence [20] and absolutely no difference in XRD patterns were observed. One of the possible reasons for difference of the microwave-assisted hydrothermal treatment's results between DyF_3 and PrF_3 nanoparticles may be the different symmetry (DyF_3 – orthorhombic D_{2h}^{16}-Pnma; PrF_3 – hexagonal C_{6v}^{3}-$P6_3cm$). Another reason could be the difference of lattice energies for lanthanide ions Pr and Dy [33].

The type of crystal structure defects is also different. In the case of PrF_3 nanoparticles—point defects, for DyF_3 nanoparticles—the defects are more severe. Annealing of the defects of the crystal structure of DyF_3 nanoparticles leads to significant (2–5 times) narrowing of XRD peaks. Usually the width of XRD peaks is related to the nanoparticles size and microstrains. There are various methods of X-ray analysis such as Scherrer [34], Williamson-Hall [35], and Warren-Averbach [36] methods. The average nanoparticles size was calculated using Debye-Scherrer's formula:

$$D = \frac{K\lambda}{\beta_{hkl}\cos\theta}. \tag{3}$$

For synthesized DyF_3 nanoparticles, the estimation gives too high values (ex., for sample #3 55 nm), which supports the defect nature of XRD peaks linewidth.

The analysis of XRD pattern by Williamson-Hall method also gives too high values for the average size of nanoparticles and attempts to estimate lattice distortions do not give reliable results. Warren-Averbach analysis is suitable for resolved XRD peaks and in our case is not applicable.

4. Conclusions

In summary, the series of DyF_3 nanoparticles was successfully synthesized by the microwave-assisted colloidal hydrothermal method for the first time. The nanoparticles were characterized by TEM and XRD. The average size of particles is about 16–18 nm and the size distribution becomes narrower after the microwave treatment. It was observed that the microwave irradiation treatment strongly affects the width of XRD peaks. They become narrower with the microwave treatment. The defect-annealing model of the microwave-assisted hydrothermal modification process is suggested.

Competing Interests

The authors declare that they have no competing interests.

Acknowledgments

The work was performed according to the Russian Government Program of Competitive Growth of Kazan Federal University. E. M. Alakshin has been financially supported by the Russian Foundation for Basic Research (Project no. 16-32-60155 mol_a_dk).

References

[1] F. Vetrone and J. A. Capobianco, "Lanthanide-doped fluoride nanoparticles: luminescence, upconversion, and biological applications," *International Journal of Nanotechnology*, vol. 5, no. 9–12, pp. 1306–1339, 2008.

[2] B. M. Tissue, "Synthesis and luminescence of lanthanide ions in nanoscale insulating hosts," *Chemistry of Materials*, vol. 10, no. 10, pp. 2837–2845, 1998.

[3] Z. G. Chen, H. L. Chen, H. Hu et al., "Versatile synthesis strategy for carboxylic acid-functionalized upconverting nanophosphors as biological labels," *Journal of the American Chemical Society*, vol. 130, no. 10, pp. 3023–3029, 2008.

[4] D. K. Chatterjee, A. J. Rufaihah, and Y. Zhang, "Upconversion fluorescence imaging of cells and small animals using lanthanide doped nanocrystals," *Biomaterials*, vol. 29, no. 7, pp. 937–943, 2008.

[5] P. R. Diamente, M. Raudsepp, and F. C. J. M. van Veggel, "Dispersible Tm^{3+}-doped nanoparticles that exhibit strong 1.4 μm photoluminescence," *Advanced Functional Materials*, vol. 17, no. 3, pp. 363–368, 2007.

[6] S. Sivakumar, P. R. Diamente, and F. C. J. M. van Veggel, "Silica-coated Ln^{3+}-doped LaF_3 nanoparticles as robust down-and upconverting biolabels," *Chemistry-A European Journal*, vol. 12, no. 22, pp. 5878–5884, 2006.

[7] X. Teng, Y. Zhu, W. Wei et al., "Lanthanide-doped Na_xScF_{3+x} nanocrystals: crystal structure evolution and multicolor tuning," *Journal of the American Chemical Society*, vol. 134, no. 20, pp. 8340–8343, 2012.

[8] V. Mahalingam, F. Vetrone, R. Naccache, A. Speghiniand, and J. A. Capobianco, "Colloidal Tm^{3+}/Yb^{3+}-doped $LiYF_4$ nanocrystals: multiple luminescence spanning the UV to NIR regions via low-energy excitation," *Advanced Materials*, vol. 21, no. 40, pp. 4025–4028, 2009.

[9] S. Sarkar, C. Hazra, and V. Mahalingam, "Bright luminescence from colloidal Ln^{3+}-doped $Ca_{0.72}Y_{0.28}F_{2.28}$ (Ln=Eu, Tm/Yb) nanocrystals via both high and low energy radiations," *Chemistry—A European Journal*, vol. 18, no. 23, pp. 7050–7054, 2012.

[10] S. Sarkar, B. Meesaragandla, C. Hazra, and V. Mahalingam, "Sub-5 nm Ln^{3+}-doped $BaLuF_5$ nanocrystals: a platform to realize upconversion via interparticle energy transfer (IPET)," *Advanced Materials*, vol. 25, no. 6, pp. 856–860, 2013.

[11] H. Dong, S.-R. Du, X.-Y. Zheng et al., "Lanthanide nanoparticles: from design toward bioimaging and therapy," *Chemical Reviews*, vol. 115, no. 19, pp. 10725–10815, 2015.

[12] P. Rahman and M. Green, "The synthesis of rare earth fluoride based nanoparticles," *Nanoscale*, vol. 1, no. 2, pp. 214–224, 2009.

[13] L. Ma, W.-X. Chen, Y.-F. Zheng, J. Zhao, and Z. Xu, "Microwave-assisted hydrothermal synthesis and characterizations of PrF_3 hollow nanoparticles," *Materials Letters*, vol. 61, no. 13, pp. 2765–2768, 2007.

[14] M. S. Tagirov, E. M. Alakshin, R. R. Gazizulin et al., "Spin kinetics of 3He in contact with synthesized PrF_3 nanoparticles," *Journal of Low Temperature Physics*, vol. 162, no. 5-6, pp. 645–652, 2011.

[15] E. M. Alakshin, B. M. Gabidullin, and A. T. Gubaidullin, "Development of various methods for PrF3 nanoparticles synthesis," https://arxiv.org/abs/1104.0208.

[16] E. M. Alakshin, A. S. Aleksandrov, A. V. Egorov, A. V. Klochkov, S. L. Korableva, and M. S. Tagirov, "Nuclear pseudoquadrupole resonance of 141Pr in Van Vleck paramagnet PrF3," *JETP Letters*, vol. 94, no. 3, pp. 240–242, 2011.

[17] E. M. Alakshin, D. S. Blokhin, A. M. Sabitova et al., "Experimental proof of the existence of water clusters in fullerene-like PrF_3 nanoparticles," *JETP Letters*, vol. 96, no. 3, pp. 181–183, 2012.

[18] E. M. Alakshin, R. R. Gazizulin, A. V. Klochkov et al., "Size effect in the (PrF_3 nanoparticles-^{3}He) system," *JETP Letters*, vol. 97, no. 10, pp. 579–582, 2013.

[19] M. S. Pudovkin, S. L. Korableva, A. O. Krasheninnicova et al., "Toxicity of laser irradiated photoactive fluoride PrF_3 nanoparticles toward bacteria," *Journal of Physics: Conference Series*, vol. 560, no. 1, Article ID 012011, 2014.

[20] E. M. Alakshin, R. R. Gazizulin, A. V. Klochkov et al., "Annealing of PrF_3 nanoparticles by microwave irradiation," *Optics and Spectroscopy*, vol. 116, no. 5, pp. 721–723, 2014.

[21] A. M. Gazizulina, E. M. Alakshin, E. I. Baibekov et al., "Electron paramagnetic resonance of Gd^{3+} ions in powders of LaF_3:Gd^{3+} nanocrystals," *JETP Letters*, vol. 99, no. 3, pp. 149–152, 2014.

[22] S.-E. Park, T.-H. Kim, S.-R. Lee, S. Namkung, and T.-S. Jang, "Effect of sintering conditions on the magnetic and microstructural properties of Nd-Fe-B sintered magnets doped with DyF_3 powders," *Journal of Applied Physics*, vol. 111, no. 7, Article ID 07A707, 2012.

[23] X. J. Cao, L. Chen, S. Guo et al., "Coercivity enhancement of sintered Nd-Fe-B magnets by efficiently diffusing DyF3 based on electrophoretic deposition," *Journal of Alloys and Compounds*, vol. 631, pp. 315–320, 2015.

[24] S. Sawatzki, I. Dirba, L. Schultz, and O. Gutfleisch, "Electrical and magnetic properties of hot-deformed Nd-Fe-B magnets with different DyF_3 additions," *Journal of Applied Physics*, vol. 114, no. 13, Article ID 133902, 2013.

[25] R. Sueptitz, S. Sawatzki, M. Moore, M. Uhlemann, O. Gutfleisch, and A. Gebert, "Effect of DyF_3 on the corrosion behavior of hot-pressed Nd–Fe–B permanent magnets," *Materials and Corrosion*, vol. 66, no. 2, pp. 152–157, 2015.

[26] Z. Duan, J. Zhang, and L. Hu, "Spectroscopic properties and Judd-Ofelt theory analysis of Dy^{3+} doped oxyfluoride silicate glass," *Journal of Applied Physics*, vol. 101, no. 4, Article ID 043110, 2007.

[27] A. V. Savinkov, S. L. Korableva, A. A. Rodionov et al., "Magnetic properties of Dy^{3+} ions and crystal field characterization in YF_3:Dy^{3+} and DyF_3 single crystals," *Journal of Physics Condensed Matter*, vol. 20, no. 48, Article ID 485220, 2008.

[28] X. Ye, J. Chen, M. Engel et al., "Competition of shape and interaction patchiness for self-assembling nanoplates," *Nature Chemistry*, vol. 5, no. 6, pp. 466–473, 2013.

[29] S. Bhowmik, T. Gorai, and U. Maitra, "A room temperature, templated synthesis of lanthanide trifluoride nanoparticles and their unusual self-assembly," *Journal of Materials Chemistry C*, vol. 2, no. 9, pp. 1597–1600, 2014.

[30] C. Li, J. Yang, P. Yang, H. Lian, and J. Lin, "Hydrothermal synthesis of lanthanide fluorides LnF_3 (Ln = La to Lu) nano-/microcrystals with multiform structures and morphologies," *Chemistry of Materials*, vol. 20, no. 13, pp. 4317–4326, 2008.

[31] W. Kraus and G. Nolze, "POWDER CELL—a program for the representation and manipulation of crystal structures and calculation of the resulting X-ray powder patterns," *Journal of Applied Crystallography*, vol. 29, no. 3, pp. 301–303, 1996.

[32] DyF3 crystal structure, Springer Materials (electronic resource), http://materials.springer.com/isp/crystallographic/docs/sd_1300541.

[33] C. Dong, M. Raudsepp, and F. Van Veggel, "Kinetically determined crystal structures of undoped and La^{3+}-doped LnF_3," *Journal of Physical Chemistry C*, vol. 113, no. 1, pp. 472–478, 2009.

[34] P. Scherrer, "Bestimmung der Grösse und der inneren Struktur von Kolloidteilchen mittels Röntgenstrahlen," *Nachrichten von der Gesellschaft der Wissenschaften zu Göttingen*, vol. 26, pp. 98–100, 1918.

[35] G. K. Williamson and W. H. Hall, "X-ray line broadening from filed aluminium and wolfram," *Acta Metallurgica*, vol. 1, no. 1, pp. 22–31, 1953.

[36] B. E. Warren and B. L. Averbach, "The separation of cold-work distortion and particle size broadening in X-ray patterns," *Journal of Applied Physics*, vol. 23, no. 4, p. 497, 1952.